

# FIELD CONTROL CHALLENGES FOR DIFFERENT LINAC TYPES

Olof Troeng\*, Dept. of Automatic Control, Lund University, Sweden  
Mamad Eshraqi, European Spallation Source ERIC, Lund, Sweden  
Anders Johansson, Dept. of EIT, Lund University, Sweden  
Sven Pfeiffer, Deutsches Elektronen-Synchrotron, Hamburg, Germany

## Abstract

Linacs for free-electron lasers typically require cavity field stabilities of 0.01% and 0.01 degree, while the requirements for high-intensity proton linacs are on the order of 0.1–1% and 0.1–1 degrees. From these numbers it is easy to believe that the field control problem for proton linacs is many times easier than for free-electron lasers linacs. In this contribution we explain why this is not necessarily the case, and discuss the factors that make field control challenging. We also discuss the drivers for field stability, and how high-level decisions on the linac design affect the difficulty of the field control problem.

## INTRODUCTION

Radio-frequency linear particle accelerators are essential components in free-electron lasers (FELs), spallation sources, accelerator-driven nuclear energy, and certain physics experiments. RF linacs accelerate charged particles with electromagnetic fields confined in radio-frequency cavities. For proper operation it is important that the amplitudes and phases of the accelerating electromagnetic fields are accurately regulated. This is achieved by fast feedback loops implemented in the so-called low-level RF system.

In this paper we discuss what factors that make the field control problem challenging. One obvious aspect is the acceptable levels of amplitude and phase errors (in % and °). However, another aspect is the amount of load disturbances. For cavities with heavy beam loading, it can be challenging to meet even modest field error specifications.

The paper is organized as follows. First, we discuss the drivers for field stability in FELs and high-intensity proton linacs. Then we consider how the cavity bandwidth determine the sensitivity to disturbances. Finally, we give examples of particular field control challenges for specific linacs. While related, we will not discuss aspects related to tuning control.

## DRIVERS FOR FIELD STABILITY

### *Free-Electron-Laser Linacs*

For FEL linacs, it is mainly beam parameters such as bunch-to-bunch energy spread, bunch compression in the injector, and the bunch arrival time at the undulator, that dictate the required field stability. The European XFEL [1] and LCLS-II [2] require field stabilities on the order of 0.01 % (rms) for the amplitude and 0.01° (rms) for the phase.

\* oloft@control.lth.se

### *High-Intensity Proton Linacs*

In proton linacs it takes a long distance before the beam velocity approaches  $c$ . Therefore it is necessary to have a synchronous phase such that the cavity fields provide longitudinal focusing (in addition to acceleration). From Gauss' law it then follows that transverse defocusing is also provided. Unless the amplitudes and phases of the fields are accurately controlled, the beam is focused differently in the longitudinal and transverse planes, causing a mismatch that leads to halo production and loss of halo particles. Proton losses on the structure cause activation which delays hands-on maintenance, and therefore availability of the accelerator. To allow hands-on maintenance (within a reasonable time) the beam losses should not exceed 1 W/m [3]. It is often challenging to achieve this level of beam loss for multi-megawatt proton accelerators. Many high-intensity proton accelerators are *beam-loss limited*, i.e., many subsystem requirements, as those on field stability, are driven by the need to limit beam losses.

## DISTURBANCE SENSITIVITY AS A FUNCTION OF CAVITY BANDWIDTH

The relative disturbance sensitivity of a cavity is determined by its resistive losses, beam loading, and external coupling (which is typically chosen based on the first two parameters). However, for brevity, we consider instead the cavity (half-)bandwidth  $\gamma$  (which is determined by the resistive losses and the external coupling).

We consider only the accelerating mode; parasitic modes can be neglected if they are mitigated by notch filters.

### *Normalized Cavity Dynamics*

We will consider the baseband dynamics of the accelerating cavity mode [4] around an operating point  $(\mathbf{V}_0, \mathbf{I}_{g0}, \mathbf{I}_{b0})$ , and normalize accordingly. To this end, introduce  $\mathbf{z}$ ,  $\mathbf{u}$ ,  $\mathbf{d}_g$ ,  $\mathbf{d}_b$  as normalized deviations from the operating point according to:  $\mathbf{V} = \mathbf{V}_0(1 + \mathbf{z})$ , where  $\mathbf{z}$  is relative field errors;  $\mathbf{I}_g = \mathbf{I}_{g0}(1 + \mathbf{d}_g) + \gamma/(\omega_0(r/Q)/2)\mathbf{u}$ , where  $\mathbf{u}$  corresponds to control action, and  $\mathbf{d}_g$  to amplifier ripple; and  $\mathbf{I}_b = \mathbf{I}_{b0}(1 + \mathbf{d}_b)$ , where  $\mathbf{d}_b$  is relative beam variations. The normalized deviations satisfy

$$\frac{dz}{dt} = (-\gamma + i\Delta\omega)\mathbf{z} + \gamma\mathbf{u} + \gamma(\mathbf{K}_g\mathbf{d}_g + \mathbf{K}_b\mathbf{d}_b), \quad (1)$$

where  $\Delta\omega$  is the detuning,  $\mathbf{K}_g := \omega_0(r/Q)\mathbf{I}_{g0}/(2\gamma V_0)$ , and  $\mathbf{K}_b := \omega_0(r/Q)\mathbf{I}_{b0}/(4\gamma V_0)$ . For optimally tuned and coupled cavities  $\mathbf{K}_g$  is real, and  $1 \leq \mathbf{K}_g \leq 2$ , and  $|\mathbf{K}_b| \lesssim 1$ . See Table 1 for typical values of  $\mathbf{K}_g$  and  $|\mathbf{K}_b|$ .

Table 1: Parameters that affect field-control performance for some different cavities, together with the required amplitude stability (the required phase stabilities are similar). The first three cavities are superconducting, and the last two are normal conducting.

Cavity type (facility)	$\gamma$ kHz	$K_g$ -	$ K_b $ -	req. % (rms)
TESLA (LCLS-II)	0.016	1.5	0.5	0.01
TESLA (XFEL)	0.14	2.0	1.0	0.01
Medium- $\beta$ (ESS)	0.7	1.9	1.0	0.1
DTL (ESS)	12	1.3	0.3	0.2
RFQ (ESS)	61	1.1	0.2	0.2

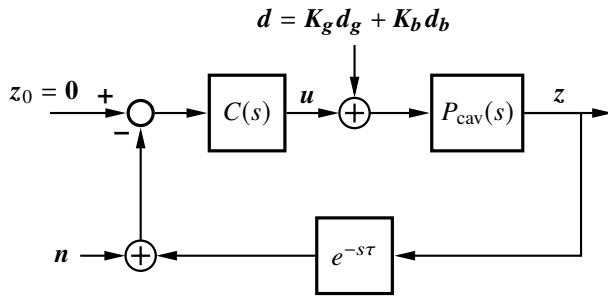


Figure 1: Block diagram for a field control loop operating around a nominal operating point;  $z$  denotes (normalized) field errors,  $n$  denotes measurement noise, and  $d$  denotes load disturbances.

Note that  $z = 0.01 + 0.02i$  corresponds to a field error of  $\approx 1\%$  in amplitude, and  $\approx 0.02 \text{ rad} \approx 1.1^\circ$  in phase. The situation is similar for  $d_g$  and  $d_b$ .

From (1) we see that the transfer function from  $u$  to  $z$ , and also the transfer function from load disturbances  $d := K_g d_g + K_b d_b$  to  $z$ , is given by

$$P_{\text{cav}}(s) := \frac{\gamma}{s + \gamma - i\Delta\omega}. \quad (2)$$

### Typical Cavity-Field-Controller Design

A reasonable transfer function model of the field control loop is

$$L(s) = C(s)P_{\text{cav}}(s)e^{-s\tau},$$

where  $P_{\text{cav}}(s)$  is given by (2),  $\tau$  is the loop delay, and  $C(s)$  is the controller transfer function, see Figure 1. In our example we will assume  $\tau = 1 \mu\text{s}$ , and that the load disturbances  $d$  have a low-frequency spectrum  $D(s) = 1/s$ .

The control objective is to minimize field errors (rms). Neglecting the impact of measurement noise, this corresponds to minimization of  $\|z\|_2 = \|P_{\text{cav}}SD\|_2$ , where  $S := 1/(1 + PC)$  is the so-called sensitivity function. To avoid issues with amplifier nonlinearity, as well as transversal kick [5], we also impose the constraint  $\|CS\|_2 \leq 30$ , which corresponds to less than  $\approx 30 \text{ dB}$  amplification of white measurement noise to the control signal. To ensure closed-loop

robustness, we impose the constraint  $\max_{\omega} |S(i\omega)| \leq 1.6$ , which guarantees a phase margin  $\text{PM} \geq 36^\circ$ . To keep the analysis simple, we consider controllers of the form  $C(s) = K(1 + 1/(sT_i))/(sT_f + 1)$ , i.e., proportional-integral controllers with first-order filters that limit amplification of high-frequency noise. Optimizing the controller parameters with respect to the given objective and constraints, for different bandwidths  $\gamma$ , gives the closed-loop transfer functions in Figure 2. The selected  $\gamma$  values correspond to the first four rows of Table 1.

### Discussion

From the magnitude plot of  $G_{un}$  in Figure 2 we see that the lower bandwidth a cavity has, the higher the amplification of measurement noise in the field control loop is. For the high-bandwidth cavities the constraint  $\|G_{un}\|_2 \leq 30$  is not active, but for the low-bandwidth cavities, in particular for the LCLS-II cavity, this constraint forces a significant reduction of the closed-loop bandwidth (as indicated the sensitivity function  $S$ ). This leads to reduced low-frequency disturbance rejection.

Another important observation can be made from the magnitude plot of  $G_{zd}$ , namely, that high-bandwidth cavities have many times greater sensitivity to disturbances than low-bandwidth cavities. To a smaller extent, the sensitivity to amplifier ripple and beam ripple is also determined by the coefficients  $K_g$  and  $K_b$  in (1).

It should be recalled that our analysis in this section concerns the *sensitivity* to disturbances, and that the field errors are also proportional to the relative magnitude of the disturbances. For example, it is typically economically and technically more challenging to achieve low phase ripple for megawatt klystrons and modulators, than for lower-power solid-state amplifiers.

To summarize: field control loops with low-bandwidth cavities are sensitivity to measurement noise, while those with high-bandwidth cavities are sensitive load disturbances. This explains why significant engineering effort has gone into the design of the LCLS-II LLRF system; and why it can be harder to achieve field errors of 0.2% for high-bandwidth, normal-conducting cavities, than to achieve 0.01% for superconducting cavities.

## ACCELERATOR SPECIFIC CHALLENGES

Finally, we would like to give some examples of field-control challenges that have arisen from the high-level design of specific linacs. Table 2 contains operation parameters for the considered linacs [1, 6–8].

### Free-Electron-Laser Linacs

**The European XFEL** [1] Hamburg, Germany was built for high brilliance and X-ray-wavelengths. To make the linac economically feasible, each RF amplifier powers *thirty-two* superconducting TESLA cavities [9, 10]. Given the 140 Hz-bandwidth of the cavities, it is clear that calibration and tuning control need careful consideration. There are

Content from this work may be used under the terms of the CC BY 3.0 licence (© 2019). Any distribution of this work must maintain attribution to the author(s), title of the work, publisher, and DOI

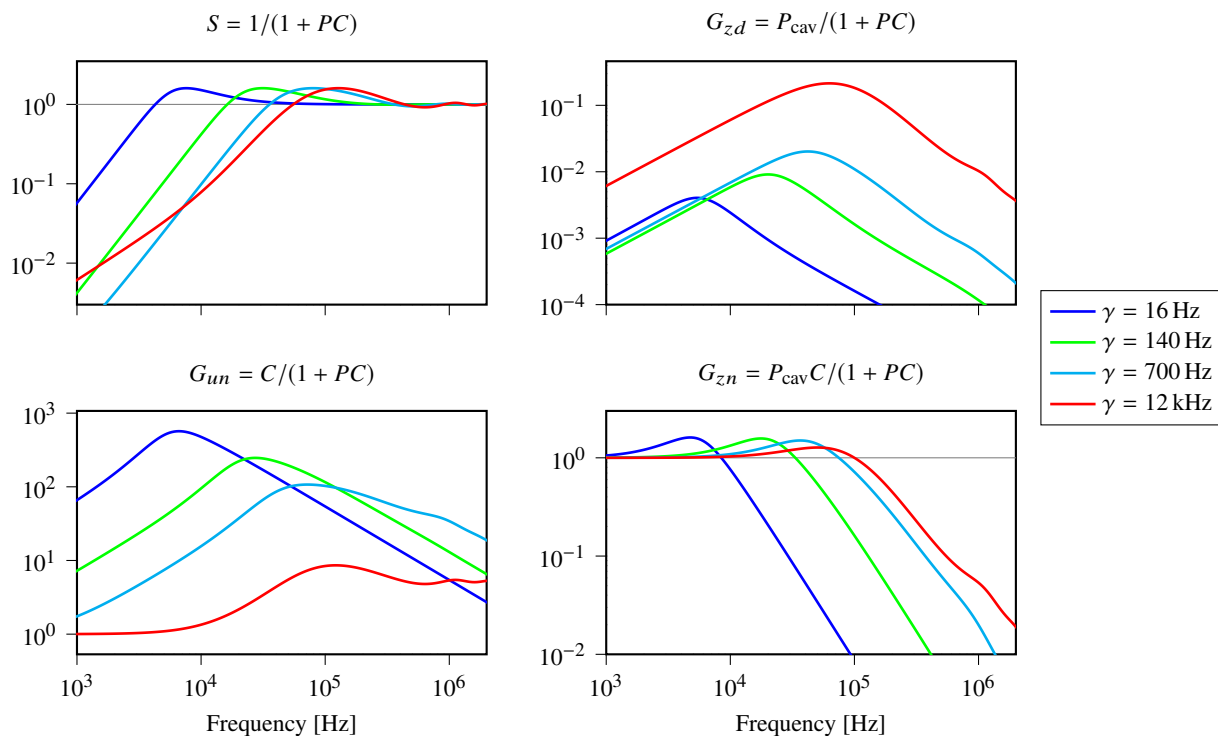


Figure 2: Bode magnitude plots of the transfer functions known as the gang of four. These plots capture the essential closed-loop, frequency-domain characteristics of a feedback interconnection. Note that the amplification of measurement noise to the control signal ( $G_{un}$ ) is more problematic, the lower bandwidth a cavity has. Conversely, the impact of load disturbances is most severe for high-bandwidth cavities, as indicated by  $G_{zd}$ .

Table 2: Parameters for the Discussed Linacs [1, 6–8]. The linac at the European Spallation Source is considered as an example of a high-intensity proton linac.

	European XFEL	LCLS-II	Swiss-FEL	ESS
Final Energy [GeV]	17.5	4	5.8	2
Beam Current* [mA]	5	0.3	†	62.5
Pulse Length [ms]	0.65	CW	†	2.86
Pulse Frequency [Hz]	10	CW	100	14
Peak Beam Power* [MW]	100	1.2	†	125
Avg. Beam Power [MW]	0.6	1.2	†	5
Bunch frequency (during pulse) [MHz]	4.5	~1.0	†	352.21

\* Averaged over the flat-top of the RF pulse.  
 † Up to two 200 pC electron bunches per RF pulse.

additional feedback challenges in the control of the electron gun and the third-harmonic cavities.

**Linac Coherent Light Source II** [6] Stanford, CA will have a superconducting linac operating in CW mode, with a bunch repetition rate of almost 1 MHz. The cavities will have bandwidths of about 16 Hz, and will be driven by dedicated solid-state amplifiers. The low bandwidth calls for field control by self-excited loops, and makes tuning control a challenge [2].

**SwissFEL** [7] Villigen, Switzerland was designed to be an affordable, compact, and energy efficient X-ray FEL.

Its operation principle is very different from the two previous FELs—the RF pulses are extremely short, and at most two electron bunches are accelerated during each RF pulse. The RF pulses are too short for intra-pulse feedback, so it is necessary with pulse-to-pulse corrections and accurate temperature control of the normal-conducting accelerating structures [11].

### High-Intensity Proton Linacs

The gradual increase in particle velocity means that different cavity types need to be used along the linac. Often, frequency doubling is necessary to make the cavity sizes manageable. It is also common use several different types of RF amplifiers. These aspects contribute to making the control problem heterogeneous.

Due to the high beam loading, the cavity bandwidths  $\gamma$  are relatively large (see Table 2). As seen from Figure 2, this makes the cavities sensitive to disturbances. Certain ion sources have significant levels of beam-current ripple, which acts as a problematic load disturbance.

## CONCLUSION

We have given an overview of why cavity field control is important for different types of RF linacs, and discussed how the bandwidth of an accelerating cavity affects the achievable field stability. Some particularly interesting field control challenges for specific linacs were also touched upon.

## REFERENCES

- [1] M. Altarelli *et al.*, “The European X-ray free-electron laser, technical design report”, Deutsches Elektronen-Synchrotron, Tech. Rep. DESY 2006-097, 2007.
- [2] L. Doolittle *et al.*, “The LCLS-II LLRF system”, in *Proc. 6th Intl. Particle Accelerator Conf.*, 2015.
- [3] N. V. Mokhov and W. Chou, Eds., *Beam Halo and Scraping — Proc. 7th ICFA Mini-Workshop on High-Intensity and High-Brightness Hadron Beams*, 1999.
- [4] T. Schilcher, “Vector sum control of pulsed accelerating fields in Lorentz force detuned superconducting cavities”, PhD thesis, Hamburg University, 1998.
- [5] T. Hellert and M. Dohlus, “Detuning related coupler kick variation of a superconducting nine-cell 1.3 GHz cavity”, *Phys. Rev. Accel. Beams*, vol. 21, p. 042 001, 4 Apr. 2018.
- [6] J. Galayda, “The new LCLS-II project: Status and challenges”, in *Proc. 5th Intl. Particle Accelerator Conf.*, 2014.
- [7] C. Milne *et al.*, “SwissFEL: The swiss X-ray free electron laser”, *Applied Sciences*, vol. 7, no. 7, p. 720, 2017.
- [8] R. Garoby *et al.*, “The european spallation source design”, *Physica Scripta*, vol. 93, no. 1, p. 014 001, Dec. 2017.
- [9] C. Schmidt, “RF system modeling and controller design for the european XFEL”, PhD thesis, TU Hamburg-Harburg, 2010.
- [10] S. Pfeiffer, “Symmetric grey box identification and distributed beam-based controller design for free-electron lasers”, PhD thesis, TU Hamburg-Harburg, 2014.
- [11] A. Rezaeizadeh, “Automatic control strategies for the Swiss free electron laser”, PhD thesis, Swiss Federal Institute of Technology in Zurich, 2016.